Resonance Frequencies and Sound Absorption of Helmholtz Resonators With Multiple Necks

F. Langfeldt*, H. Hoppen, W. Gleine

Department of Automotive and Aeronautical Engineering, Hamburg University of Applied Sciences, Berliner Tor 7a, D–20099 Hamburg, Germany

Abstract

A new analytical model is proposed to calculate the resonance frequency and the input impedance of a Helmholtz resonator with multiple necks. Such resonators occur in practice, for example, when leaks are introduced as additional necks inside the wall of the resonators. The model uses a lumped representation of the air volumes enclosed by the necks to derive an explicit formula for the resonance frequency. Using this formula, it can be explained that the low reactance of the air volumes inside leaks of thin-walled Helmholtz resonators leads to the strong increase of the resonance frequency, as observed in previous studies. The results of the analytical model are validated with the help of experimental data available in the literature and impedance tube measurements. The analytical model as well as the measurements clearly show, that even small holes in the Helmholtz resonator lead to a significant increase in the resonance frequency and the absorption performance can be considerably reduced. The simple model can be applied to design Helmholtz resonators with multiple necks or estimate the impact of leaks.

Keywords: helmholtz resonator, resonance, leak, absorption

1. Introduction

Helmholtz resonators are widely applied in many different noise control environments for the reduction of low-frequency sound. Typically, Helmholtz resonators are used as side branches in ducts or pipes in order to mitigate sound propagation along the waveguide [1]. Other applications involve Helmholtz resonators, for example, as sound absorbers in room acoustics [2], for improving sound transmission loss of aircraft sidewalls [3] or payload fairings [4], and as acoustic metamaterials exhibiting negative effective bulk modulus [5]. The resonance frequency of a Helmholtz resonator is primarily determined by the size of the cavity volume and the neck geometry (cross-sectional area and length). In the literature, numerous recent studies have investigated the impact of different aspects of the resonator geometry on the acoustic performance of Helmholtz resonators (e.g. [6–10]).

*Corresponding author

Email addresses: Felix.Langfeldt@haw-hamburg.de (F. Langfeldt), Hannah.Hoppen@haw-hamburg.de (H. Hoppen), Wolfgang.Gleine@haw-hamburg.de (W. Gleine)

Post-print submitted to Applied Acoustics *October 5, 2018*

Please cite as: Langfeldt, F., Hoppen, H. and W. Gleine. Resonance frequencies and sound absorption of Helmholtz resonators with multiple necks. *Applied Acoustics* 145 (2019): 314–319. https://doi.org/10.1016/j.apacoust.2018.10.021

Another critical aspect for the acoustical properties of Helmholtz resonators is the ability of the cavity to sustain the high sound pressure levels that occur inside the cavity at resonance. Photiadis [11], for example, has shown that a Helmholtz resonator with elastic cavity walls exhibits a reduced resonance frequency and bandwidth, as compared to a rigid cavity. Selamet et al. [12] have investigated both experimentally and computationally the effect of leaks and gaps (i.e. additional necks) in Helmholtz resonators. They observed that the resonance frequency is increased and the peak transmission loss can be greatly reduced when additional necks are introduced into the internal baffle of a Helmholtz resonator. The same effect can be observed when the necks are introduced on the outer surface of the resonator [13]. Since in many practical applications, leaks or gaps in Helmholtz resonators cannot be avoided due to manufacturing tolerances [12] or are even necessary, e.g. to allow drainage of moisture accumulating inside the cavity [3], it is important to understand and take into account the impact of multiple necks in the design of Helmholtz resonators.

This contribution provides a simple theoretical model of the acoustical properties of Helmholtz resonators with multiple necks. In contrast to the extensive multi-dimensional boundary element model presented by Selamet et al. [12], the proposed model, based upon a lumped representation of the resonator parts, provides an explicit formula for the resonance frequency and input impedance of such resonator configurations. It can therefore be employed to better understand and quickly estimate the impact of multiple necks (e.g. due to leaks) in different Helmholtz resonator configurations.

2. Theory

Consider the Helmholtz resonator depicted in Fig. 1. The resonator consists of a cavity with the volume V_0 and a total of N necks connected to the cavity. Each neck i, with $1 \leq i \leq N$, is characterized by a neck length l_i and a cross-sectional area S_i. As indicated by the shaded areas in Fig. 1, every neck encloses a

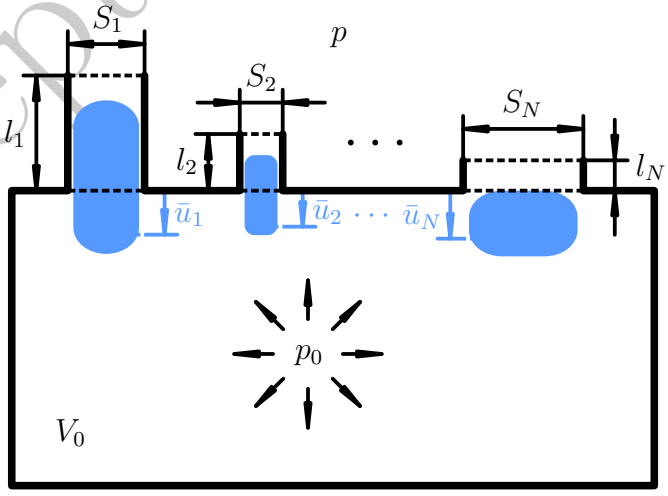

Figure 1: Schematic representation of a Helmholtz resonator with multiple necks. Here, only three necks are shown for clarity, but the number of necks N can be any integer number $N \geq 1$. The shaded areas represent the fluid volumes that are enclosed by the resonator necks.

certain fluid volume which acts as a mass resting upon the spring stiffness of the cavity volume V_0. The average displacements $\bar{u}_i$ of the neck air volumes (with the positive direction of $\bar{u}_i$ defined as pointing inside the cavity) lead to a volume change $\Delta V_i = -S_i \bar{u}_i$ of the cavity volume V_0. This volume change causes a compression of the fluid inside the cavity resulting in a pressure amplitude p_0, which can be substantially different to the pressure amplitude p outside the cavity. It is assumed that the dimensions of the Helmholtz resonator cavity are smaller than the acoustic wavelength at the resonance frequency. Thus, p_0 can be assumed to be uniform inside the cavity and calculated with the bulk modulus of the fluid $\rho_0 c_0^2$ according to [14, p. 192] as

$$p_0 = -\rho_0 c_0^2 \frac{\Delta V}{V_0} = -\frac{\rho_0 c_0^2}{V_0} \sum_{i=1}^{N} \Delta V_i = \frac{\rho_0 c_0^2}{V_0} \sum_{i=1}^{N} S_i \bar{u}_i, \tag{1}$$

where ρ_0 and c_0 are the density and speed of sound of the fluid inside the cavity.

The average displacements $\bar{u}_i$ of the neck air volumes are related to the pressure difference $\Delta p = p - p_0$ via the acoustic impedance of the necks Z_i as follows:

$$Z_i = \frac{\Delta p}{\mathrm{i}\omega \bar{u}_i} = \frac{p - p_0}{\mathrm{i}\omega \bar{u}_i}, \tag{2}$$

where, assuming a harmonic time dependency of the form $\exp(\mathrm{i}\omega t)$, $\mathrm{i}\omega \bar{u}_i$ corresponds to the average velocity of the neck air volumes. Rearranging Eq. (2) and substituting Eq. (1) for p_0 yields the following coupled equations for the displacements in each resonator neck:

$$\mathrm{i}\omega Z_i \bar{u}_i = p - p_0 = p - \frac{\rho_0 c_0^2}{V_0} \sum_{j=1}^{N} S_j \bar{u}_j. \tag{3}$$

This can also be expressed in matrix form as the system of equations

$$\left(\mathrm{i}\omega \begin{bmatrix} Z_1 & & \\ & \ddots & \\ & & Z_N \end{bmatrix} + \frac{\rho_0 c_0^2}{V_0} \begin{bmatrix} S_1 & \cdots & S_N \\ \vdots & \ddots & \vdots \\ S_1 & \cdots & S_N \end{bmatrix} \right) \begin{pmatrix} \bar{u}_1 \\ \vdots \\ \bar{u}_N \end{pmatrix} = \begin{pmatrix} p \\ \vdots \\ p \end{pmatrix}. \tag{4}$$

For the further analysis it is convenient to decompose the neck impedance Z_i into a resistance part R_i and a reactance part ωM_i as

$$Z_i = R_i + \mathrm{i}\omega M_i, \tag{5}$$

where R_i describes the damping due to viscous losses in the acoustic boundary layer and M_i can be interpreted as the inertial mass of the neck air volume. Typically, both quantities depend on the shape of the neck, the neck integration on the resonator, and the fluid properties. In the case of cylindrical necks with diameter d_i, the neck air volume mass M_i can be approximated as

$$M_i = \rho_0 \left(l_i + \alpha_i d_i \right), \tag{6}$$

where α_i is the so-called end correction coefficient, taking into account the inertia of a certain fluid volume surrounding the neck [12]. Thus, Eq. (4) can be rewritten as

$$\left(-\omega^2\mathbf{M} + \mathrm{i}\omega\mathbf{D} + \mathbf{C}\right)\bar{\mathbf{u}} = p\mathbf{1}, \tag{7}$$

with the mass matrix $\mathbf{M} = \mathrm{diag}(M_1, \ldots, M_N)$, damping matrix $\mathbf{D} = \mathrm{diag}(R_1, \ldots, R_N)$, stiffness matrix $\mathbf{C} = (\rho_0 c_0^2/V_0)\mathbf{1}\mathbf{1}^T\mathbf{S}$, $\mathbf{1} = (1, \ldots, 1)^T$, $\mathbf{S} = \mathrm{diag}(S_1, \ldots, S_N)^T$, and $\bar{\mathbf{u}} = (\bar{u}_1, \ldots, \bar{u}_N)$.

For the calculation of the resonance frequencies of the Helmholtz resonator, the damping matrix $\mathbf{D}$ and the outside pressure amplitude p are neglected. Therefore, the resonance frequencies ω_0 can be obtained as the eigenvalues ω_0^2 solving the eigenvalue problem

$$\underbrace{\frac{\rho_0 c_0^2}{V_0}\mathbf{M}^{-1}\mathbf{1}\mathbf{1}^T\mathbf{S}}_{\mathbf{A}}\bar{\mathbf{u}}_0 = \omega_0^2\bar{\mathbf{u}}_0. \tag{8}$$

Since the system matrix $\mathbf{A}$ is a N-by-N matrix of rank one, it has $N-1$ eigenvalues with $\omega_0^2 = 0$ and one non-zero eigenvalue with $\omega_0^2 = (\rho_0 c_0^2/V_0)\mathbf{1}^T(\mathbf{S}\mathbf{M}^{-1})\mathbf{1}$ [15]. Consequently, a Helmholtz resonator with multiple necks exhibits one non-zero resonance frequency at

$$f_0 = \frac{c_0}{2\pi}\sqrt{\frac{\rho_0}{V_0}\mathbf{1}^T(\mathbf{S}\mathbf{M}^{-1})\mathbf{1}} = \frac{c_0}{2\pi}\sqrt{\frac{\rho_0}{V_0}\sum_{i=1}^{N}\frac{S_i}{M_i}}. \tag{9}$$

It should be noted that the zero eigenvalues and corresponding eigenvectors can be interpreted physically as different stationary airflows through the Helmholtz resonator with no net volume change (i.e. a certain volume flow flowing in through one set of perforations and leaving the resonator cavity through the other perforations). These stationary modes have no particular influence on the acoustic properties of the Helmholtz resonator at non-zero frequencies.

In order to evaluate the acoustic performance of the Helmholtz resonator, the input impedance Z has to be determined. This quantity is defined as

$$Z = \frac{p}{v}, \tag{10}$$

i.e. the ratio of the acoustic pressure amplitude and the particle velocity on top of the resonator (see Fig. 1). At low frequencies, the surface particle velocity v can be obtained from the continuity of flow through the perforations as

$$v = \frac{\mathrm{i}\omega}{S_0}\sum_{i=1}^{N} S_i\bar{u}_i = \frac{\mathrm{i}\omega}{S_0}\mathbf{1}^T\mathbf{S}\bar{\mathbf{u}}, \tag{11}$$

where S_0 is the total area of all necks. The neck volume displacements $\bar{\mathbf{u}}$ are calculated from solving the

system of equations (7), which, after several algebraic steps, yields for Z the expression

$$Z = \frac{S_0}{\mathrm{i}\omega \mathbf{1}^T \mathbf{S} \left(-\omega^2 \mathbf{M} + \mathrm{i}\omega \mathbf{D} + (\rho_0 c_0^2 / V_0) \mathbf{1}\mathbf{1}^T \mathbf{S}\right)^{-1} \mathbf{1}} = \frac{S_0}{\sum\limits_{i=1}^{N} \frac{S_i}{Z_i}} + \frac{S_0}{\mathrm{i}\omega} \frac{\rho_0 c_0^2}{V_0}. \tag{12}$$

Note that Eq. (12) is applicable if all necks are connected to the exterior fluid domain with pressure p. In the case that, for example, only the primary neck ($i = 1$) is connected to the exterior fluid domain, the expression changes to

$$Z = \frac{S_0}{\left(\frac{S_1}{Z_1}\right)} + \frac{S_0}{\sum\limits_{i=2}^{N} \frac{S_i}{Z_i} + \mathrm{i}\omega \frac{V_0}{\rho_0 c_0^2}} \tag{13}$$

and $S_0 = S_1$. In general, the denominator of the left summand of Eq. (13) contains the summation of S_i/Z_i for all necks connected to the exterior fluid domain, while the summation in the right summand is over all necks not connected to it. The neck surface area S_0 is obtained from the areas of all necks connected to the exterior fluid.

Fig. 2 shows two typical applications of Helmholtz resonators in noise reduction. Fig. 2(a) illustrates a Helmholtz resonator acting as a silencer on a duct. In this case, the transmission loss TL can then be calculated via

$$\mathrm{TL} = -10 \lg \left| \frac{p_\mathrm{t}}{p_\mathrm{i}} \right|^2 = 20 \lg \left| 1 + \frac{1}{2} \frac{S_0}{S} \frac{\rho_0 c_0}{Z} \right|, \tag{14}$$

where S is the cross-sectional area of the duct [16]. The usage of Helmholtz resonators as sound absorbers on a rigid wall is shown in Fig. 2(b). The absorption coefficient α can be obtained using the so-called matching

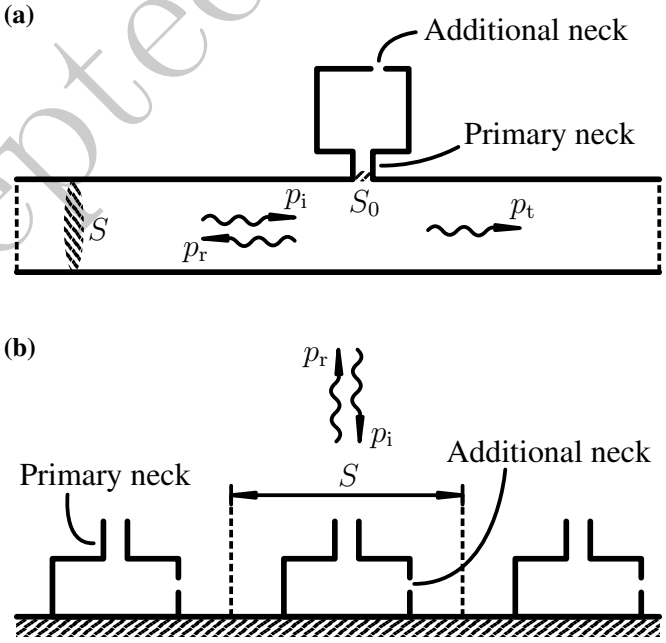

Figure 2: Illustration of different Helmholtz resonator configurations for noise reduction. (a) Silencer on a duct with transmission loss TL given by Eq. (14); (b) Sound absorber on a rigid wall with sound absorption coefficient α given by Eq. (15).

law from

$$\alpha = 1 - \left|\frac{p_\mathrm{r}}{p_\mathrm{i}}\right|^2 = \frac{4\rho_0 c_0 \frac{S}{S_0} Z_\mathrm{Re}}{\left(\frac{S}{S_0} Z_\mathrm{Re} + \rho_0 c_0\right)^2 + \frac{S^2}{S_0^2} Z_\mathrm{Im}^2}, \tag{15}$$

where S is the surface area of the resonator unit cell and Z_Re and Z_Im denote the real and imaginary parts, respectively, of Z [16].

3. Results and discussion

The proposed theoretical model for calculating the resonance frequency of a Helmholtz resonator with multiple necks via Eq. (9) is validated using experimental data available in the literature. Table 1 provides an overview of the resonator and neck parameters in the experiments. The neck diameter and length d_1 and l_1, respectively, are attributed to the primary neck of the resonator. d_2 and l_2, on the other hand, represent the geometry of the additional necks in the resonator walls (which, in this context, can be understood as leaks) and N_leaks is the number of investigated leaks, so that the total number of necks is given by $N = N_\mathrm{leaks} + 1$. In the theoretical calculations, $\rho_0 = 1.2$ kg/m^3, $c_0 = 343$ m/s, and $\eta_0 = 18.5$ µPa s are specified for the air density, speed of sound, and dynamic viscosity, respectively. According to [12], end correction coefficients of $\alpha_1 = 0.6133$ for the primary neck and $\alpha_2 = 0.8271$ for the additional necks are prescribed. The resistance parts R_i of the necks are obtained using the analytical formulas given by Maa [17].

Fig. 3 shows a comparison of the analytical values from Eq. (9) and the measured resonance frequencies by Selamet et al. [12], who investigated the acoustic properties of a Helmholtz resonator with different numbers of additional necks within the resonator baffle. The results from Eq. (9) are in very good agreement with the experimental values and confirm the dramatic effect of additional necks on the resonance frequency of a Helmholtz resonator. It should be noted that the Helmholtz resonator investigated by Selamet et al. [12] employed necks extending into the inside of the cavity. Although this design is geometrically different from the configuration showed in Fig. 1 (where the necks extend to the outside of the cavity), the good agreement between the analytical predictions and the experimental results demonstrate that the proposed model can also accurately predict the resonance frequencies of Helmholtz resonators with necks extending to the inside of the cavity. In addition, the dashed line in Fig. 3 indicates the calculated resonance frequencies, if the surface area of the additional necks is simply added to the surface area of the primary neck, i.e. $f_0 = c_0/(2\pi)\sqrt{(S_1 + N_\mathrm{leaks} S_2)/(V_0 M_1)}$. This clearly shows that it is not accurate to account for the additional

Table 1: Summary of experimental setups for Helmholtz resonators with multiple necks.

Experiment	V_0	d_1	l_1	d_2	l_2	N_leaks
Selamet et al. [12]	3071	36	89	5	1.4	0–13
Lee et al. [13]	1761	48	104	2.5–10	2	0–1
Present work	33.5	5.5	28	0.5–2	0.4	0–1
	cm^3	mm	mm	mm	mm	

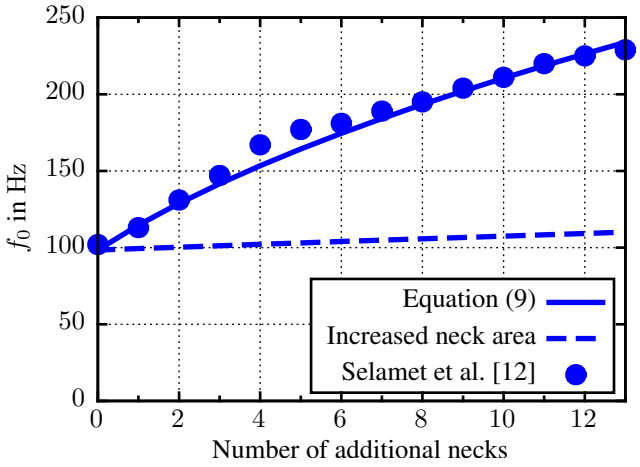

Figure 3: Comparison of the analytical results with the experimental data by Selamet et al. [12] for the resonance frequencies of a Helmholtz resonator with different numbers of additional necks.

necks in the Helmholtz resonator walls by simply adding the combined surface area of the additional necks to that of the primary neck, as already pointed out by Selamet et al. [12].

In fact, Eq. (9) provides a simple explanation for the inaccuracy of this approach: The summation over all necks does not only include the surface areas of all resonator openings, but also the reciprocals of M_i, i.e. the neck air volume masses. This can be physically understood as the effective mass of all necks combined being a parallel connection of the individual neck masses M_i, weighted by the factor $1/S_i$. In such a parallel assembly of masses, the lowest individual mass value dominates the effective mass of the whole system. Since leaks typically occur at the relatively thin walls of a resonator, their throat length l_i is in most cases much smaller than that of the primary neck. Thus, resonator leaks have a significantly lower air volume mass than the primary neck and therefore have a considerable effect on the Helmholtz resonance frequency, as observed in Fig. 3.

Fig. 4 shows experimental results from Lee et al. [13] and the corresponding theoretical results for a Helmholtz resonator with a single additional neck (i.e. $N = 2$ necks in total) and different diameters of this additional neck ranging from 0 to 10 mm (see Table 1). In these investigations, the additional neck is located on the bottom of the cavity, opposite to the location of the primary neck (similar to what is shown in Fig. 2(a)). This is different to the situation illustrated in Fig. 1, but since the acoustic wavelength generally is much larger than the resonator dimensions, the acoustic pressure inside the cavity can be assumed to be uniform and it can be expected that the neck positions are not significantly affecting the resonance frequencies. For this case, a good agreement between the predictions of Eq. (9) and the experimental data can be observed as well. If very small diameters of the second neck are considered, the frequency increase is small because the area S_2 is proportional to d_2^2 and therefore diminishes the effect of the low air volume mass in the second neck. If $d_2 > l_2$, however, the resonance frequency increases considerably as the second neck diameter becomes larger.

Finally, it should be noted that Eq. (9) can be expressed in a more compact form by introducing the

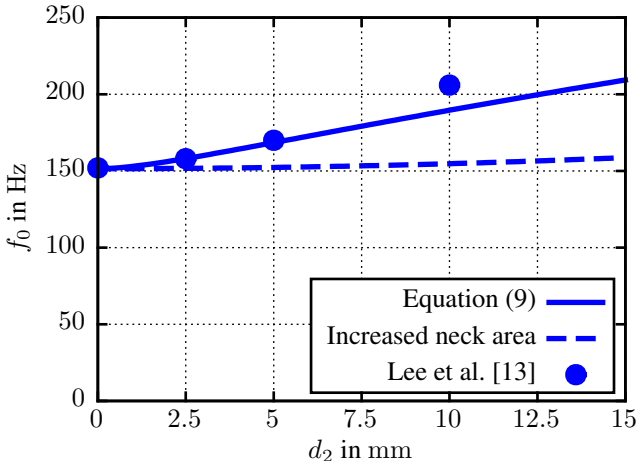

Figure 4: Comparison of the analytical results with the experimental data by Lee et al. [13] for the resonance frequencies of a Helmholtz resonator with two necks and different diameters d_2 of the second neck.

resonance frequencies $f_i = c_0/(2\pi)\sqrt{\rho_0 S_i/(V_0 M_i)}$, which correspond to the Helmholtz resonance frequencies with all, except the i-th, openings closed. Thus, Eq. (9) becomes

$$f_0 = \sqrt{\sum_{i=1}^{N} f_i^2} = \sqrt{f_1^2 + f_{\text{leaks}}^2}, \tag{16}$$

where, in addition to f_1, the resonance frequency f_{leaks} has been defined as the resonance frequency of the resonator with only the primary neck ($i = 1$) closed:

$$f_{\text{leaks}} = \frac{c_0}{2\pi}\sqrt{\frac{\rho_0}{V_0}\sum_{i=2}^{N}\frac{S_i}{M_i}}. \tag{17}$$

Eq. (16) shows that the resonance frequency of a Helmholtz resonator with multiple necks (e.g. primary neck and additional necks due to leaks) is given by the square root of the sum of the squared resonance frequency without leaks f_1^2 and the squared resonance frequency with leaks only f_{leaks}^2. Since the geometry of leaks typically is such (i.e. small neck length) that the resulting Helmholtz resonance frequency is relatively high, they will contribute significantly to the radicand in Eq. (16). Therefore, leaks in thin-walled resonators always increase the resonance frequency f_0 compared to the case with only the primary neck f_1. Fig. 5 illustrates the shifting of f_0 relative to f_1 for different values of f_{leaks}/f_1. It can be seen that additional necks always lead to an increase of the Helmholtz resonance frequency, especially when $f_{\text{leaks}} > f_1$. In order to keep the Helmholtz resonance frequency relatively unchanged, it is, on the other hand, required that $f_{\text{leaks}} \ll f_1$. For example, to achieve a resonance frequency f_0 which is at most 10 % higher than f_1, the frequency f_{leaks} must be below 46 % of the value of f_1. In the case of the resonator investigated by Selamet et al. [12], this would require an additional neck diameter of $d_2 \leq 3.1$ mm.

The effect of multiple necks on the sound absorption of a Helmholtz resonator has been studied using

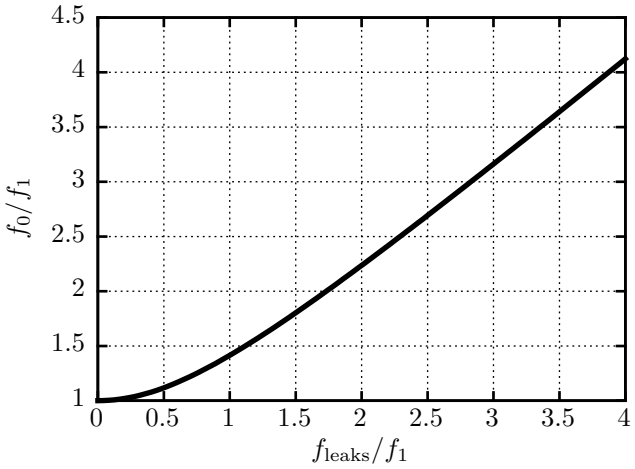

Figure 5: Shifting of the Helmholtz resonance frequency f_0 compared to the resonance frequency without additional necks f_1 for different values of f_{leaks}/f_1.

impedance tube measurements with a two-microphone setup according to ISO 10534-2. Fig. 6(a) shows a schematical drawing of the experimental setup with the impedance tube. The diameter of the tube was given by $D = 100$ mm, so that $S = 0.25\pi D^2 = 78.54$ cm^2. The test sample was a spherical resonator with a diameter of 40 mm and a wall thickness of $l_2 = 0.4$ mm (see Table 1). A neck with $d_1 = 5.5$ mm and $l_1 = 28$ mm was attached on top of the resonator. Additional necks were realized through drilled holes in the Helmholtz resonator cavity. The diameter of the holes varied from $d_2 = 0.5$ to 2 mm. A photograph of the Helmholtz resonator is shown in Fig. 6(b). In order to measure the sound absorption coefficient α, the resonator sample was attached to the rigid back wall of the tube using putty (similar to the absorber configuration shown in Fig. 2(b)).

The influence of the hole diameter on the absorption behavior of the Helmholtz resonator and the resonance frequency is depicted in Fig. 7. The lines show the analytical absorption coefficient from Eq. (15), while the symbols represent the impedance tube measurements. Overall, the analytically calculated absorption coefficient is corresponding well with the measured values. Besides the increase of the resonance frequency, holes with a small diameter $d_2 < 2$ mm also lead to a significant loss in absorption. The absorption coefficient is reduced because of damping effects arising at the acoustic boundary layer of the holes. The viscous

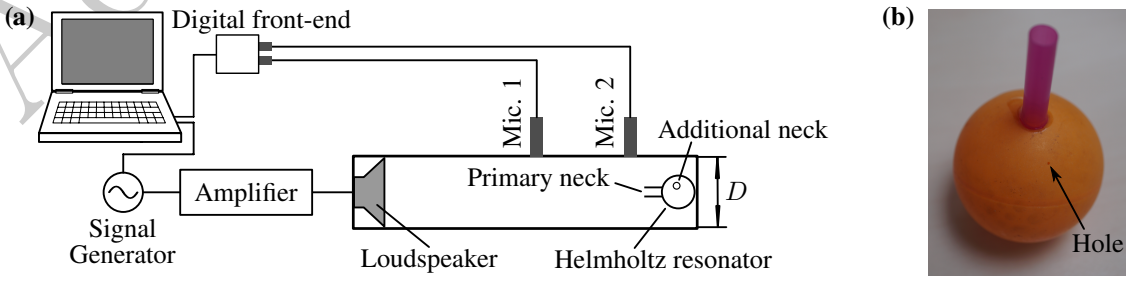

Figure 6: Illustration of the experimental setup for the sound absorption measurement of a Helmholtz resonator with multiple necks. (a) Drawing of the impedance tube setup with the Helmholtz resonator attached to the tube back wall; (b) Photograph of the resonator used in the experiments with a hole in the resonator wall acting as the second neck.

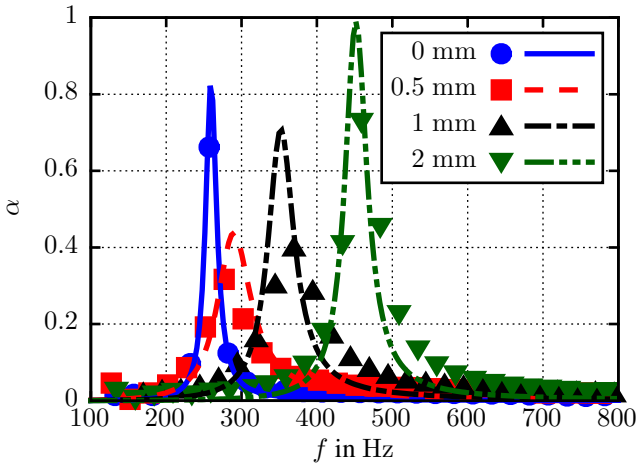

Figure 7: Comparison of the analytically calculated and experimentally measured absorption coefficients α of a Helmholtz resonator with two necks and different diameters d_2 of the second neck.

boundary layer between 250 and 350 Hz has a thickness of $\delta_\mathrm{v} = \sqrt{2\eta_0/\omega} = 0.12$ to 0.14 mm [18] and is therefore relatively large compared to the small hole diameter of $d_2 = 0.5$ mm to 1 mm. These large boundary layers lead to high resistive parts of the neck impedance, reducing the absorption coefficient according to Eq. (15).

It is to observe, that the calculated resonance frequencies of the Helmholtz resonator with the additional neck having a diameter d_2 greater than 0.5 mm do slightly underestimate the measured resonance frequency, while the calculated absorption coefficient overestimates the measured absorption coefficient. This can be attributed to inaccuracies in the modelling of the resistance of the second neck using the model by Maa [17]. In general, however, Fig. 7 confirms the drastic increase of resonance frequency due to the additional neck and shows that small holes have an undesired effect on the absorption behavior of Helmholtz resonators.

In order to further investigate the influence of the additional neck on the sound absorption, Fig. 8 shows the real and imaginary parts of the input impedance Z of the Helmholtz resonator calculated using Eq. (12) for the different values of d_2. The curves in Fig. 8 indicate the normalized input impedance $(S/S_0)Z/(\rho_0 c_0)$, which is equal to unity if the sound absorption is 100 % (i.e. the impedance is perfectly matched to the characteristic impedance of the surrounding fluid) and the imaginary part is zero at the maxima of the absorption spectrum (i.e. at the Helmholtz resonance).

In the case of no additional neck (i.e. $d_2 = 0$ mm), the real part of the normalized Helmholtz resonator input impedance, as shown in Fig. 8(a), is between 1.5 and 4 within the frequency range of interest. Therefore, the corresponding absorption peak in Fig. 7 is quite high, but $\alpha = 1$ cannot be achieved. If the additional neck is introduced with a very small diameter of $d_2 = 0.5$ mm, the real part of Z increases rapidly to much higher values. Due to the high resistance of small perforations (R_i is proportional to $1/d_i^2$ [17]), the impedance matching to the incident sound wave becomes poorer and the maximum absorption coefficient is reduced. As soon as d_2 is further increased, the real part of Z is reduced, because the resistance of the additional neck diminishes. For $d_2 = 2$ mm, the curve for Z_Re is below that of the Helmholtz resonator

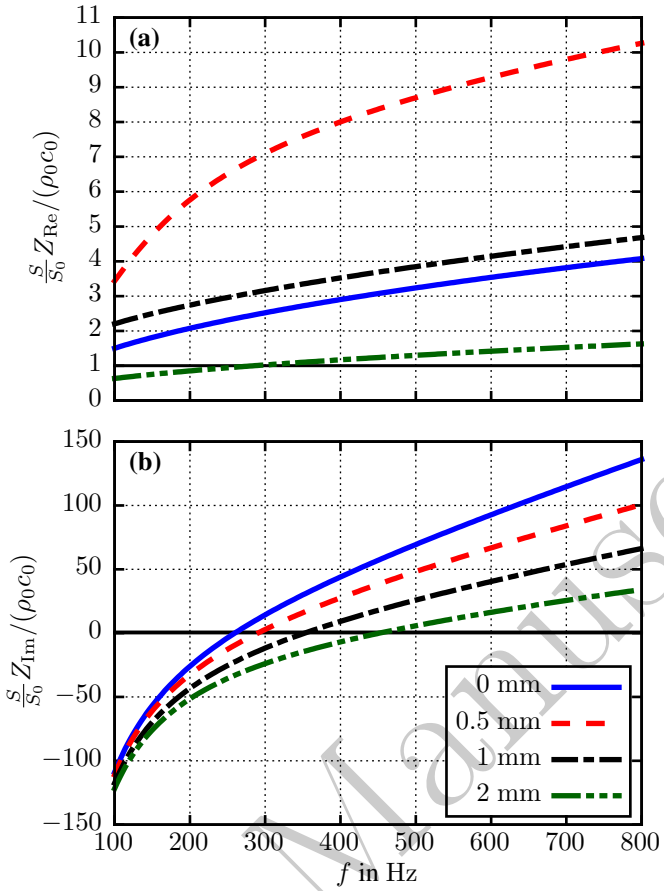

Figure 8: Normalized input impedance Z of the experimentally investigated Helmholtz resonator with two necks and different diameters d_2 of the second neck calculated using Eq. (12). (a) Real part; (b) Imaginary part.

without additional neck and close to the optimum value of $(S/S_0)Z_{\mathrm{Re}}/(\rho_0 c_0) = 1$. Thus, due to the larger open surface introduced by the additional neck, the impedance matching is improved and the absorption coefficient reaches nearly $\alpha = 1$.

For the imaginary part of the normalized impedance shown in Fig. 8(b), it can be seen that each increase of the additional neck diameter d_2 reduces the slope of the curve. Consequently, the frequencies for which $Z_{\mathrm{Im}} = 0$ (corresponding to the Helmholtz resonance frequencies) are increased. This is in line with the previous results within this section, that additional necks always lead to an increase of the Helmholtz resonance frequency.

4. Conclusions

In the present contribution, a theoretical model for predicting the resonance frequency and the input impedance of a Helmholtz resonator with multiple necks has been presented. The resulting explicit equations can be applied to estimate and physically understand the effect of leaks (i.e. additional necks) on the acoustic performance of Helmholtz resonators. Experimental data available in the literature was used to validate the proposed model. It could be shown that additional necks in the Helmholtz resonator walls always lead to

an increase of the resonance frequency of the resonator. By analyzing the resulting equation (9) it could be shown, that the small neck length of the leaks in thin-walled resonators and the corresponding small effective mass of these additional necks is primarily responsible for the significant impact of additional necks on the resonance frequency. This result can be used in the design of Helmholtz resonators, for which leaks or gaps cannot be fully avoided.

In addition to that, the impact of multiple necks on the sound absorption of Helmholtz resonators has been investigated using the theoretical model and impedance tube measurements. The analytical and experimental investigations clearly showed the increase of the Helmholtz resonator resonance frequency due to a small additional neck. Furthermore, small holes with a relatively large acoustic boundary layer compared to the hole dimensions lead to a reduced absorption behavior of the Helmholtz resonator.

Acknowledgements

This work has been performed under the framework of the research projects New Acoustic Insulation Metamaterial Technology for Aerospace (NAIMMTA), funded by the Federal Ministry of Education and Research [grant number: 03INT504AB], and Flight-LAB, funded by the Federal Ministry for Economic Affairs and Energy [grant number: 20K1511D]. The financial support is gratefully acknowledged by the authors.

References

[1] K. Chen, Y. Chen, K. Lin, C. Weng, The improvement on the transmission loss of a duct by adding helmholtz resonators, Appl. Acoust. 54 (1998) 71–82.

[2] A. Cummings, The effects of a resonator array on the sound field in a cavity, J. Sound Vib. 154 (1992) 25–44.

[3] D. N. May, K. J. Plotkin, R. G. Selden, B. H. Sharp, Lightweight Sidewalls for Aircraft Interior Noise Control, NASA CR-172490, 1985.

[4] I. U. Borchers, S. T. Laemmlein, P. Bartels, A. Rausch, M. Faust, J. A. F. Coebergh, K. Koeble, Acoustic protection on payload fairings of expendable launch vehicles, 1997. U.S. patent 5,670,758.

[5] Y. M. Seo, J. J. Park, S. H. Lee, C. M. Park, C. K. Kim, S. H. Lee, Acoustic metamaterial exhibiting four different sign combinations of density and modulus, J. Appl. Phys. 111 (2012) 023504.

[6] N. Dickey, A. Selamet, Helmholtz resonators: One-dimensional limit for small cavity length-to-diameter ratios, J. Sound Vib. 195 (1996) 512–517.

[7] A. Selamet, I. Lee, Helmholtz resonator with extended neck, J. Acoust. Soc. Am. 113 (2003) 1975–1985.

[8] X. Shi, C. M. Mak, Helmholtz resonator with a spiral neck, Appl. Acoust. 99 (2015) 68–71.

[9] C. Cai, C.-M. Mak, X. Shi, An extended neck versus a spiral neck of the helmholtz resonator, Appl. Acoust. 115 (2017) 74–80.

[10] C. Cai, C. M. Mak, Acoustic performance of different helmholtz resonator array configurations, Appl. Acoust. 130 (2018) 204–209.

[11] D. M. Photiadis, The effect of wall elasticity on the properties of a helmholtz resonator, J. Acoust. Soc. Am. 90 (1991) 1188–1190.

[12] A. Selamet, H. Kim, N. T. Huff, Leakage effect in helmholtz resonators, J. Acoust. Soc. Am. 126 (2009) 1142–1150.

[13] I. Lee, K. Jeon, J. Park, The effect of leakage on the acoustic performance of reactive silencers, Appl. Acoust. 74 (2013) 479–484.

[14] L. L. Beranek, Acoustics, Acoustical Society of America, Woodbury, New York, 1993.

[15] J. Ding, A. Zhou, Eigenvalues of rank-one updated matrices with some applications, Appl. Math. Lett. 20 (2007) 1223–1226.

[16] M. Möser, Engineering acoustics: an introduction to noise control, Springer, Berlin, 2009.

[17] D.-Y. Maa, Theory and design of microperforated panel sound-absorbing constructions, Sci. Sinica 18 (1975) 55–71.

[18] M. R. Stinson, The propagation of plane sound waves in narrow and wide circular tubes, and generalization to uniform tubes of arbitrary crossâĂŘsectional shape, J. Acoust. Soc. Am. 89 (1991) 550–558.